COMPARING ACIP PILE CONSTRUCTION, TESTING AND DESIGN METHODS IN SAND AND CLAY

C. Vipulanandan, Ph.D., P.E. and Kalaiarasi Vembu, Ph.D
Center for Innovative Grouting Materials and Technology (CIGMAT)
Department of Civil and Environmental Engineering
University of Houston, Houston, TX 77204-4003
Phone: (713) 743-4278

Abstract: Construction curing and axial behavior of Auger Cast in Place (ACIP) Piles in very dense sand and hard clay were studied using instrumented piles. Installation procedure and the quality of the material used in the construction have significant effects on the behavior of the ACIP piles. The maximum and minimum pressure required to advance the auger during construction was monitored with time. Also the construction quality was monitored using the automated monitoring system where the volume of grout pumped and the pressures were monitored with depth. The volume ratio and pumping pressures were monitored at every 1 m (3 ft) lift during grouting. The curing of the pile was monitored using axial vibrating wire strain gages at four levels and lateral vibrating wire strain gages at two levels. The residual strain and temperature profile in the curing pile was monitored over a period of week to determine the appropriate time for load testing the piles.

Load tests were performed on 760 mm (30 in.) diameter and 10 m (33 ft) long ACIP piles in dense sand and 12 m (36 ft) long pile in hard clay. The load-settlement and load transfer relationships of the piles were investigated based on the load test results. Development of skin friction in the load test piles and the reaction piles in very dense sand and hard clay were also investigated. In order to better quantify the performance of ACIP piles in sand and clay, additional load tests were investigated with the data obtained from the CIGMAT-ACIP database. A non-dimensional hyperbolic relationship was used to verify the non linear load displacement behavior of full scale load test data in sand and clay.

Introduction

Augered cast-in-place piles (ACIP) are drilled foundation installed by drilling a hole with a continuous flight auger to a predetermined depth. The equipments and techniques of ACIP piles have evolved since the 1940s (Neate, 1988). These piles have been used in the private sector in the United States since the mid 1940s (O'Neill, 1994) and became very popular in the early 1990's because of the developments in the construction quality control systems. ACIP piles are typically installed with diameters ranging from 0.3 to 1.0 m and lengths up to 30 m (Brown, 2005) although longer lengths have occasionally been installed. Compared to the drilled shafts and driven piles, ACIP piles can be installed more rapidly with relatively less disturbances to the surroundings in favorable geological condition. In general non-displacement piles carry most of the applied load by shaft friction under the working load and design load and the magnitude of the skin friction depends on the soil type, construction method and the loading type. Hence the load

displacement and load transfer behavior of piles in compression and tension in very dense sand and hard clay soil were studied. The development of side resistance in compression and tension for the load test piles and the reaction pile and end resistance in load test piles were also investigated.

Objective:

The main objective of this study was to compare the differences and similarity in ACIP piles installation and performance in dense soil and hard clay.

a. Site information

Full scale load tests were performed on two ACIP piles for two bridges at East Cochino Bayou (ECB) and Cochino Bayou (CB) on SH7 near Lufkin, Texas. The ECB site and the CB site were quarter mile apart from each other along SH7 and was located approximately 30 miles east of Crockett, Texas.

i. ***East Cochino Bayou, ECB (Sand Site)***

The site was located in the Crockett formation (mixed soil profile for 40 to 150 m (125 to 450 ft.) thick with soft clays, unconsolidated fine-grained sands, and red soil) which is an Eocene-aged deposit under Clairborne group. The bridge site consisted of sandy soil profiles from loose to very dense sand. The top layer was loose sand to a depth of 5 m (17 ft) and underlied by a 2.8 m (9 ft) thick dense sand layer. Very dense sand layer was located at a depth of 7 m (26 ft) and gave most of the carrying capacity of the test pile. Test pile was 10 m (33.1 ft) long and almost 3 m (10 ft) of the pile was socketed into the dense sand layer. Figure 1 shows the instrumentation and geotechnical profile of ECB and the results from the Texas Cone Penetrometer.

ii. ***Cochino Bayou, CB (Clay Site)***

The Cochino Bayou bridge site consists of a mixed soil profile of generally soft to stiff clays and loose sands. The top layer was loose gravelly sand to a depth of 3 m (10 ft) and underlied by a 5 m (16.5 ft) thick very soft clay layer. Stiff clay layer was located starting from the depth 8.5 m (27.5 ft) and resulted in carrying the most capacity of the test pile. The test pile was 12 m (39.1) ft long and almost 5.5 m (18 ft) length of pile was socketed into this layer. Figure 2 shows the instrumentation and geotechnical profile of CB.

b. Pile Installation Monitoring

Construction quality was monitored using the automated monitoring system where the volume of grout pumped and the pressures are monitored with depth. One of the main concerns when using the ACIP piles is the possibility of decompression of soil surrounding the pile during augering. Control of the rate of penetration of the auger will avoid decompression of the ground, loosening of the in-situ soil, and ground subsidence. If the velocity of the auger penetration was less than the critical velocity decompression will occur (Viggiani, 1989). Hence, the maximum and minimum pressure required to advance the auger was monitored with time. The critical rate of penetration of the auger was found to be 30 mm/sec with an auger revolution of 5 rpm which was held constant during the drilling for ECB. Figure 3 shows grout line pressure measurements during the

grouting phase. Maximum grout pressure was held almost constant and was about 1380 kN/m^2 (200 psi). Minimum grout pressure was fluctuating along the depth. The average minimum pressure was higher at deeper levels due to the higher soil confinement. As shown in Figure 4, The grout ratio was equal or less than 1.15 recommended by DFI (DFI 1990) was satisfied at every depth except between the top 1-2 m (3-6 ft). Grout ratio was 0.94 at this interval and not considered a problem since about 2.5 m (8 ft) of grout head was used in the borehole. The grout pressure level is important to prevent any soil collapse during the withdrawal of the auger.

The grout line pressure measurements during the grouting phase for CB pile is shown in Figure 5. The grout pressure level is important to prevent any soil collapse during the withdrawal of the auger. The maximum and minimum grout pressures were held almost constant and were around 1655 kN/m^2 (240 psi) and 965 kN/m^2 (140 psi) respectively. Pumped grout volume was measured for every 1m (3 ft) withdrawal which was considered accurate enough to assure pile integrity. Figure 6 shows that the 1.15 grout ratio condition was satisfied.

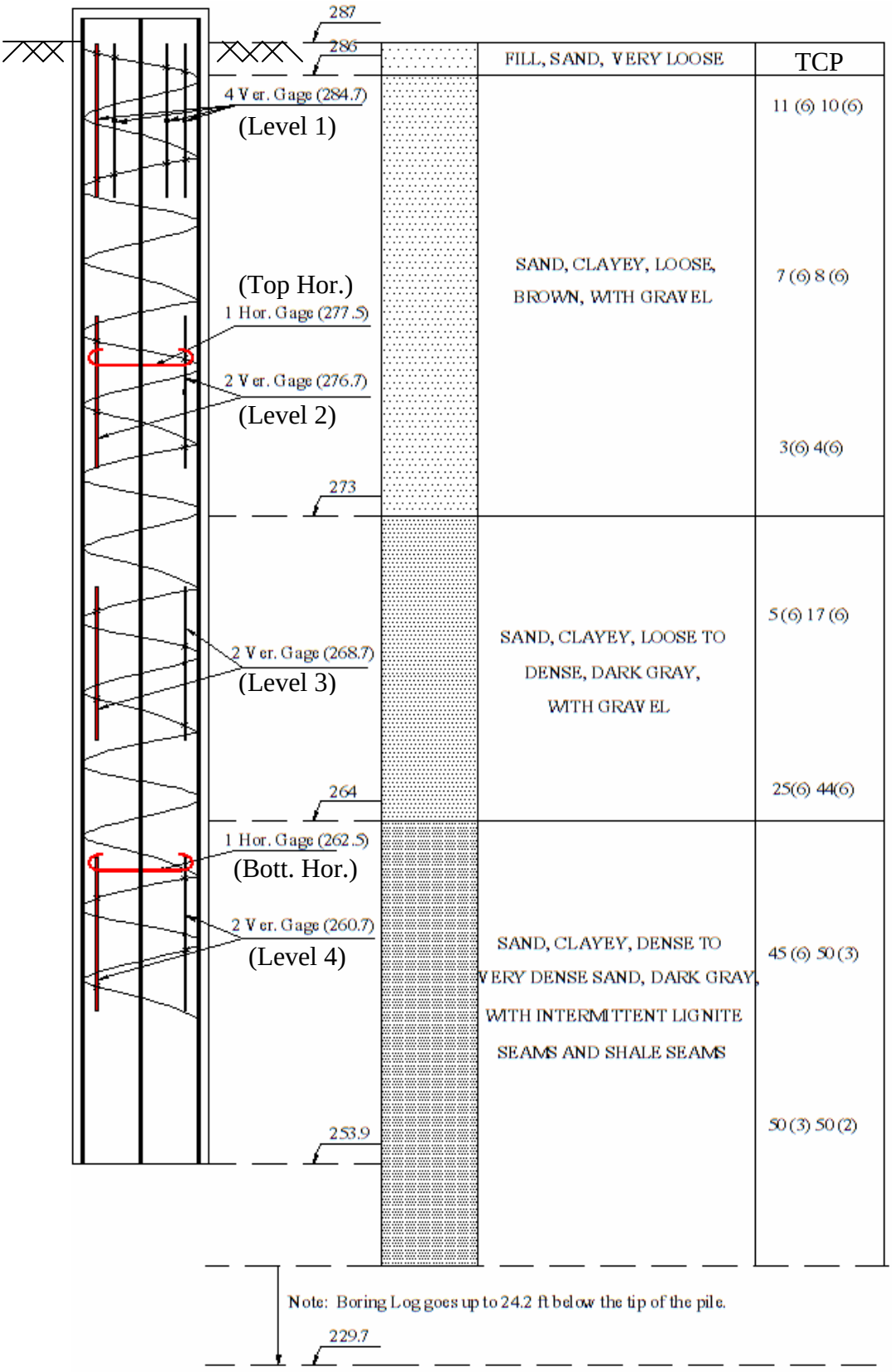

Figure 1 Instrumentation and Geotechnical Profile at ECB (Sand Site)

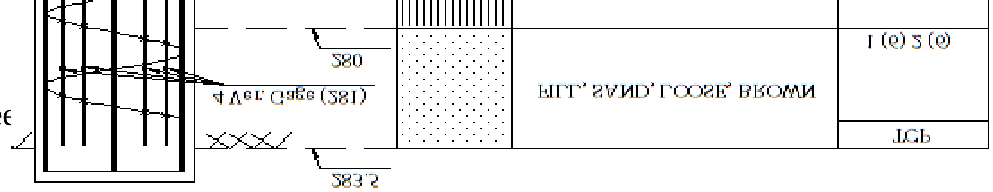

(Level 1)

(Top Hor.)

(Level 2)

(Level 3)

(Bott. Hor.)

(Level 4)

Figure 2 Instrumentation and Geotechnical Profile at CB (Clay Site)

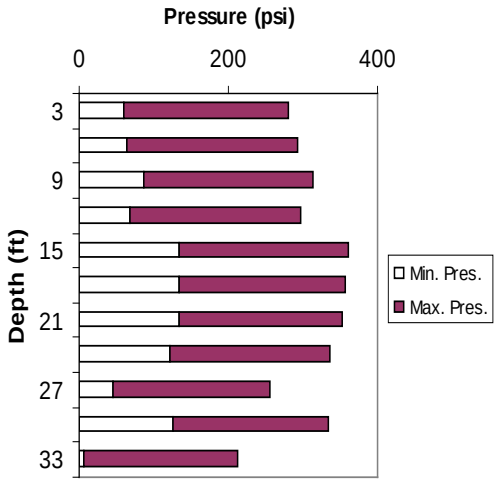

Figure 3 Applied Minimum and Maximum Grout Pressures (ECB-Sand Site)

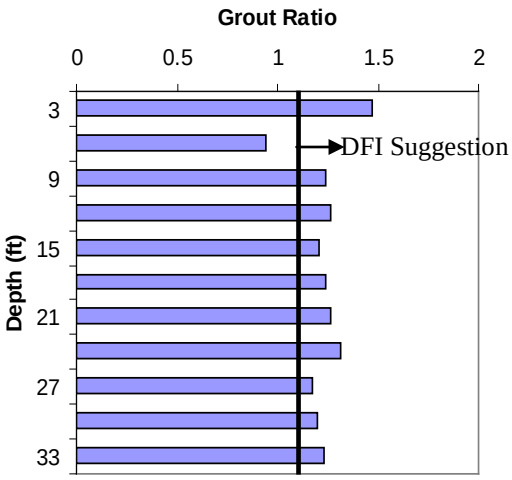

Figure 4 Pumped Grout Ratios by Depth (ECB-Sand Site)

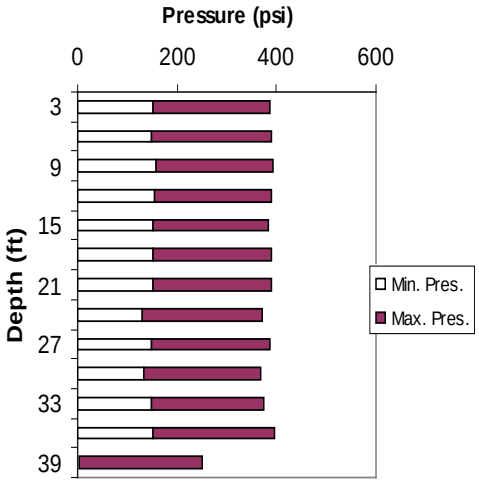

Figure 5 Pumped Grout Ratios by Depth (CB-Clay Site)

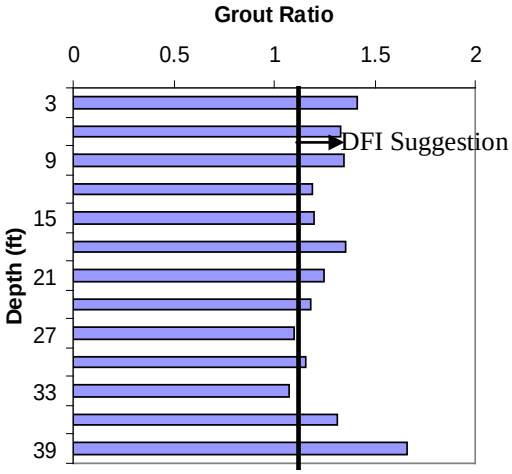

Figure 6 Applied Minimum and Maximum Grout Pressures (CB-Clay Site)

c. Monitoring the Curing

In addition to the standard quality control techniques described above, monitoring the curing phase of an ACIP pile and interpretation of results are important to better understand the development of strains in the pile. Hence, immediately after placing the instrumented cage into the grout filled hole, temperature and strain were monitored for the test piles. Valuable information was obtained for the curing stage of the piles. Both the temperature and the strains were monitored during the curing to observe the changes by time and to decide appropriate time for load testing the pile. A detailed study of pile

installation and curing of the test pile on this site was investigated by Vipulanandan, et al. 2007. Typical time-temperature relationships for ECB and CB are shown in Figures 7 (a) and (b). Maximum and average temperatures measured at ECB (sand pile) were 63.1˚C and 54.6˚C respectively. Average time to reach the maximum temperature was 8.4 hours which was very similar for all the gages. Maximum and average temperatures measured at CB (clay site) were 69.8˚C and 62.2˚C respectively. Average time to reach the maximum temperature was 9.4 hours. The maximum temperature measured was over 40˚C higher than the surrounding ground temperature.

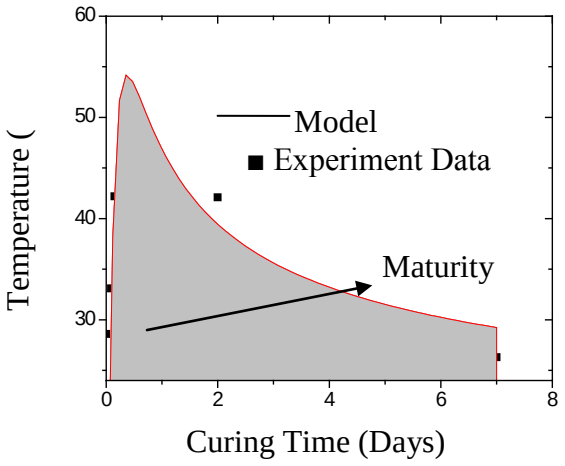

(a)

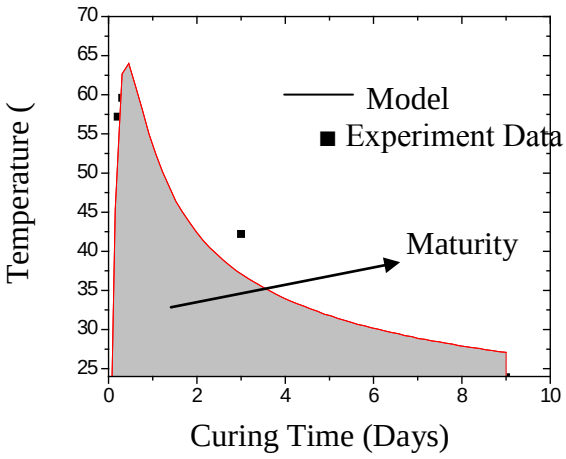

(b)

Figure 7 Typical Time-Temperature Relationship and Model Prediction (Top Level) (a) ECB (Sand Site), (b) CB (Clay Site)

d. Full Scale Load Test

In order to better characterize the behavior of ACIP piles under axial loading, two full scale load tests on instrumented ACIP piles were performed at ECB and CB. Figure 8 shows the schematic view of the load test set up. The full-scale axial load test was performed in accordance with ASTM D1143, "Standard Method of Testing Piles under Static Axial Compression load." Load was applied to the pile using a hydraulic jack acting against anchored reaction frame. Eight reaction piles (18 in. in diameter and 40 feet long) were used for each ACIP pile load test to provide adequate reactive capacity.

Pile was instrumented with load cell and head settlement gauges, in order to measure applied load and settlement during the load test. Furthermore, vibrating-wire sister bars were attached along the length of the test piles.

At ECB, pile was loaded in 10 tons increments up to 200 tons and the increment was increased to 20 tons up to 320 tons. The maximum deflection measured at the pile head was 9.14 mm (0.36 in.) at the final applied load of 320 tons and a residual displacement of 4.6 mm (0.18 in.) after unloading. The pile was unloaded in four equal steps. At CB, pile was loaded in 20 tons increments up to 520 tons. The pile was unloaded in four equal steps. The maximum deflection measured was 17.02 mm (0.67 in.) at final load of 520 tons and a residual displacement of 9.65 mm (0.38 in.) after unloading. The load settlement curve of the test pile is as shown in Figure 9. None of the test piles failed according to the Davisson criterion (Davisson, 1972). The ultimate capacity of the pile was estimated as 417 tons and 667 tons in ECB and CB respectively, based on the hyperbolic approach (Vipulanandan, 2005).

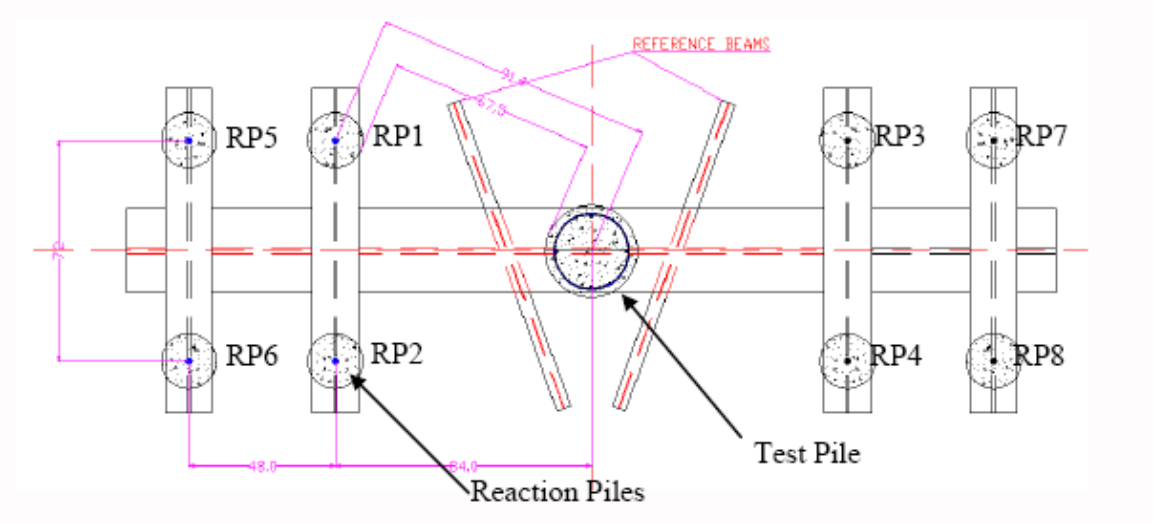

Figure 8 Schematic View of Load Test Set Up (All Dimensions are in inches)

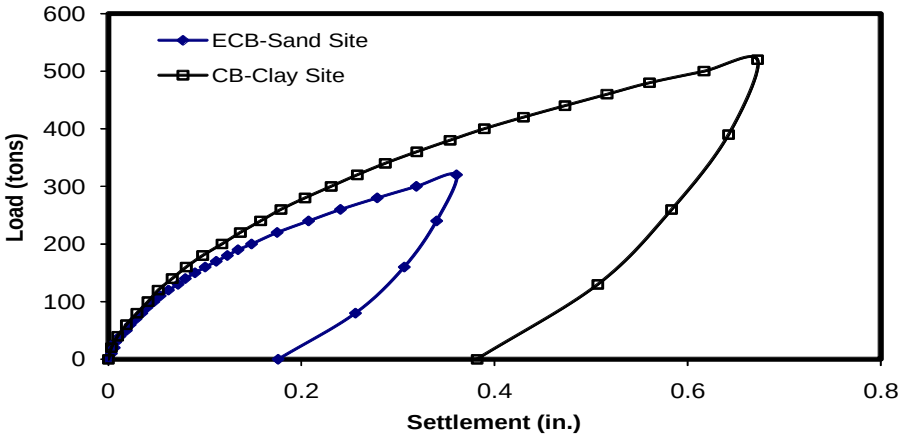

Figure 9 Load Settlement Curves

e.Load Transfer behavior

The load distribution along the length of the test piles and reaction piles were calculated based on the strain measured from the sister bars. Strain values were measured using the vibrating wire gages at four levels along the test pile and three levels along the reaction piles and the applied load at the pile head was measured using a load cell. Measured strains were converted into loads by multiplying with the axial rigidity which was back calculated using the measured data at the top of the test pile. Based on the observed curing of the grout axial rigidity was assumed to be constant all along the length of the test pile. Load on the reaction pile was determined by measuring the strain in the reinforcing bar. The load distribution relationships for the test pile and reaction pile for ECB are shown in Figures 10 and 11. The load distribution for the reaction pile is plotted for the loads applied in the test pile. The load distribution along the pile at maximum load 320 tons showed that 40.5 tons load was carried at the tip of the pile which was 13% of the total applied load. For the reaction pile the maximum load at the head was 45 tons which was 14% of the load in the compression,

The load distribution relationship for the test pile and reaction piles at CB are shown in Figures 12 and 13. The load distribution curve at maximum load 520 tons showed that 152 tons load was carried at the tip of the pile which was 29% of the total applied load. For the reaction pile the maximum load at the pile head was 54 tons which was 10.4% of the load in the compression.

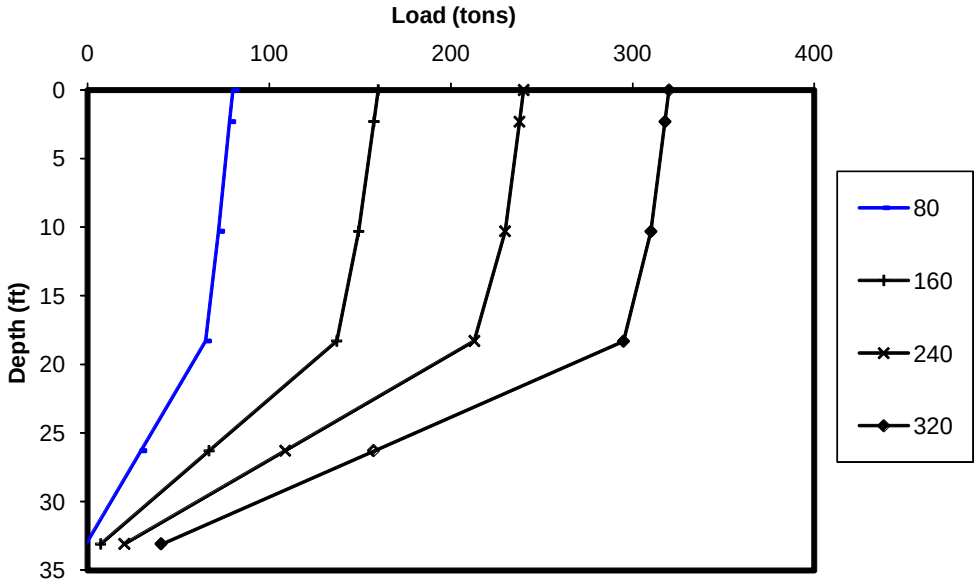

Figure 10 Load Distribution along the Test Pile – ECB (Sand Site)

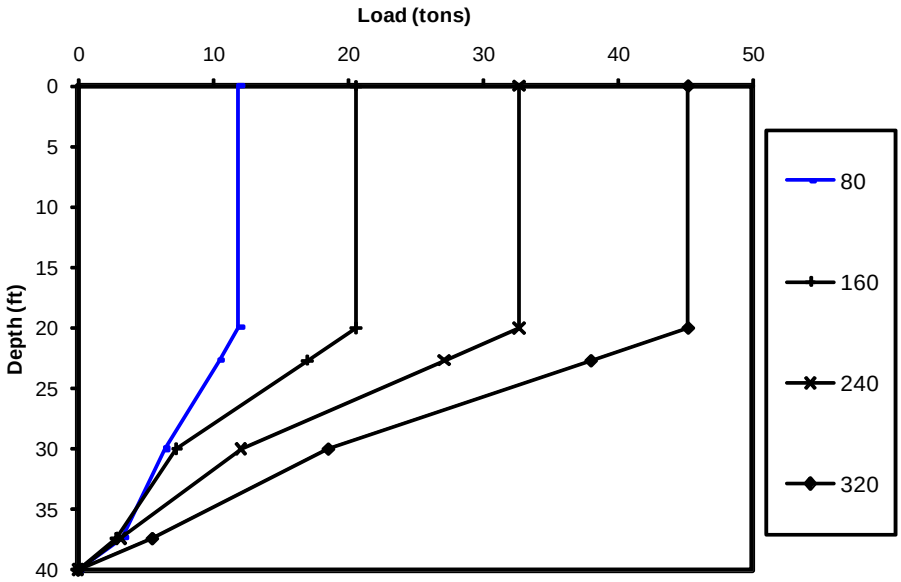

Figure 11 Typical Load Distribution along the Reaction pile – ECB (Sand Site)

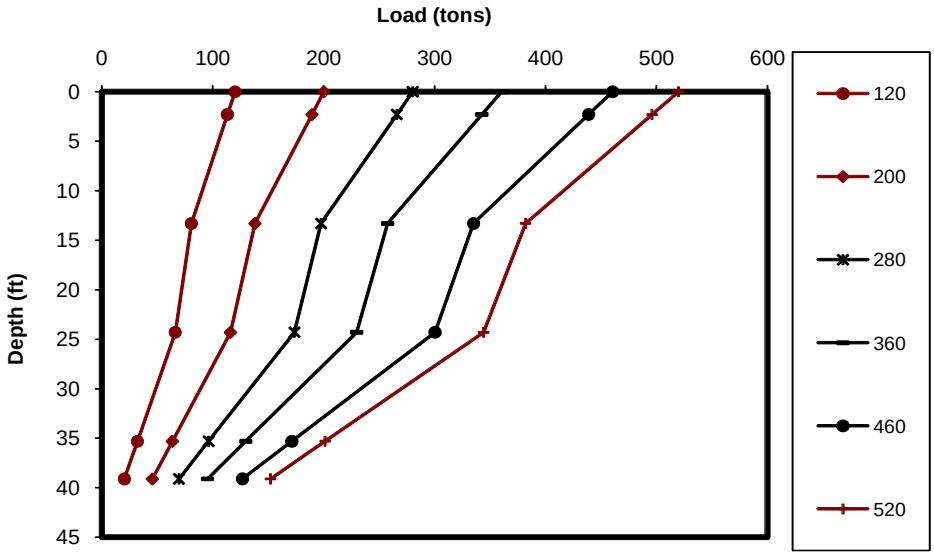

Figure 12 Load Distribution along the Test Pile – CB (Clay Site)

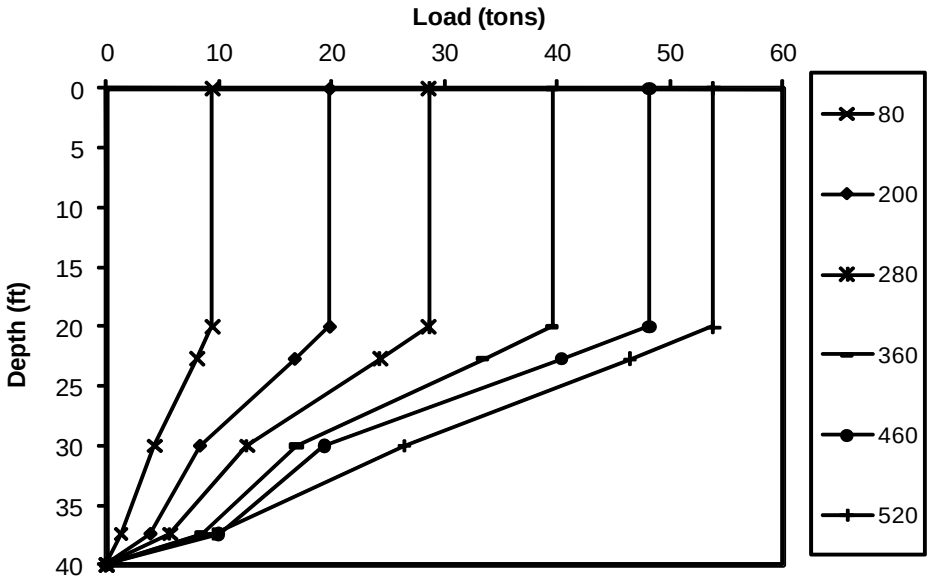

Figure 13 Typical Load Distribution along the Reaction Pile – CB (Clay Site)

Side Friction in Test Pile and Reaction Pile

East Cochino Bayou (Sand Site)

The unit load transfer relationships at selected depths along the pile for the dense sand layer was calculated from the slope of the linearly connected piecewise lines from the load distribution curve. Each of the resulting values was divided by the nominal circumference of the pile to determine unit side friction. Side friction developed in the test pile and reaction piles for ECB are compared in Figure 14. Maximum measured side friction for dense sand in the test pile was 2.2 tsf which was three times greater than maximum skin friction developed in the reaction piles. The side friction in the top segment (0-10.3 ft) and mid segment (10.3-18.3 ft) were 0.12 tsf and 0.24 tsf respectively. The ratio of side friction developed in the reaction pile (tensile) to the test piles (compressive) remained relatively constant, after the initial loading stage, around 0.25 as shown in Figure 15. The theoretical estimation of side friction considering the surface areas of the piles, based on the equivalent load carried by the test and eight reaction piles and was 0.17.

Cochino Bayou (Clay Site)

The unit load transfer relationships for CB were also calculated using the same method as described for ECB site. The side friction developed in the test pile and reaction piles for ECB were compared as shown in Figure 17. Maximum measured side friction for the hard clay in the test pile was 1.65 tsf which was twice the maximum skin friction developed in the reaction piles. The side friction in the top segment (0-13.3 ft) and mid segment (13.3-24.3 ft) were 1.3 tsf and 0.44 tsf respectively. The ratio of the side friction in the reaction pile to the test pile remained constant after the initial loading stage as shown in Figure 16. The ratio was 0.25 and 0.3 for the reaction piles RP1 and RP2 and the ratio was 0.55 for the reaction piles RP3 and RP4. The theoretical estimation of the

side friction was 0.2. The skin friction developed in the test piles are compared with the limiting capacities predicted by Wright & Reese (1979), Reese & O‟ Neill (1988) and Neely (1991) for sand layers as shown in Figure 18. The skin friction measured in the test piles were greater than the limiting capacities reported in the literature for drilled shafts.

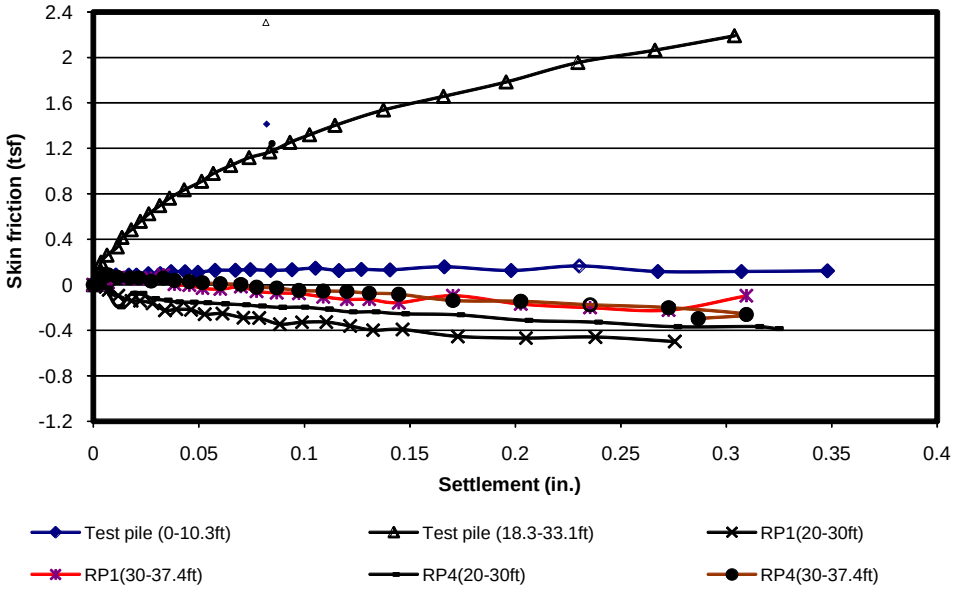

Figure 14 f-w Curves in Compression and Tension-ECB (Sand Site)

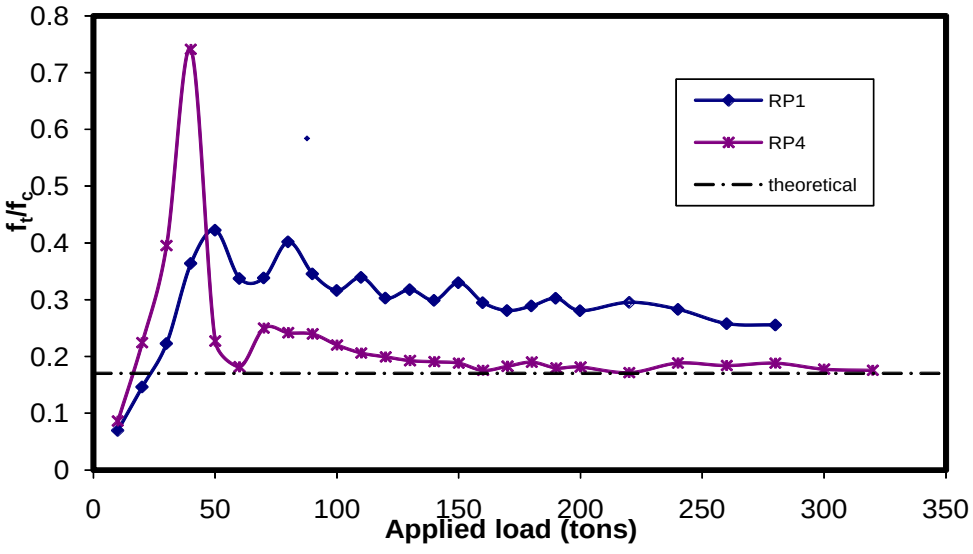

Figure 15 Side Friction Ratio in Dense Sand – ECB (Sand Pile)

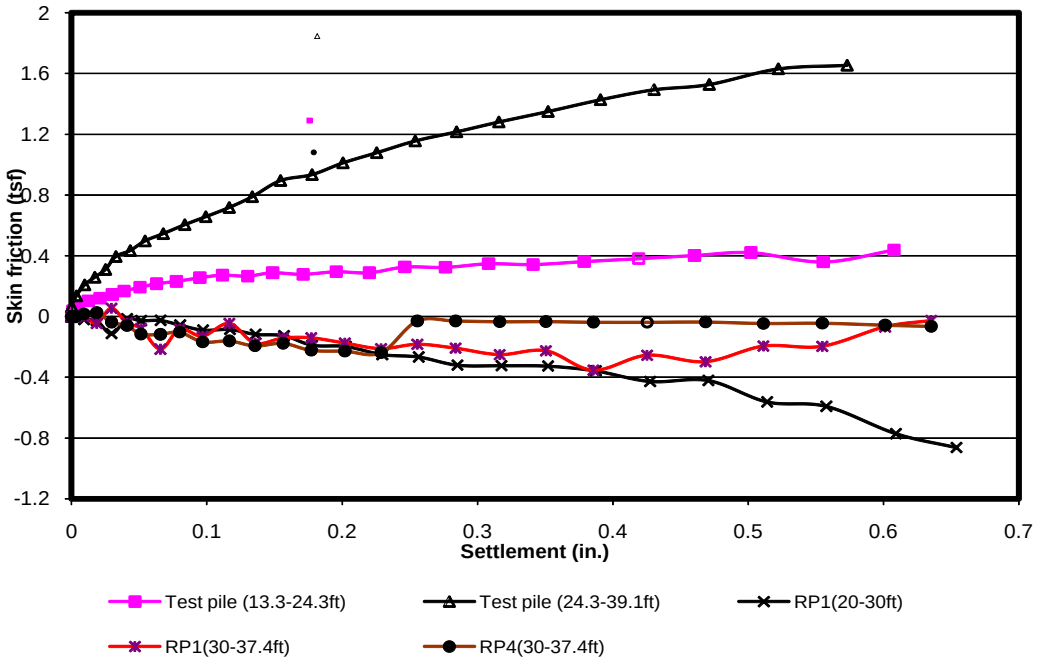

Figure 16 f-w Curves in Compression and Tension-CB (Clay Site)

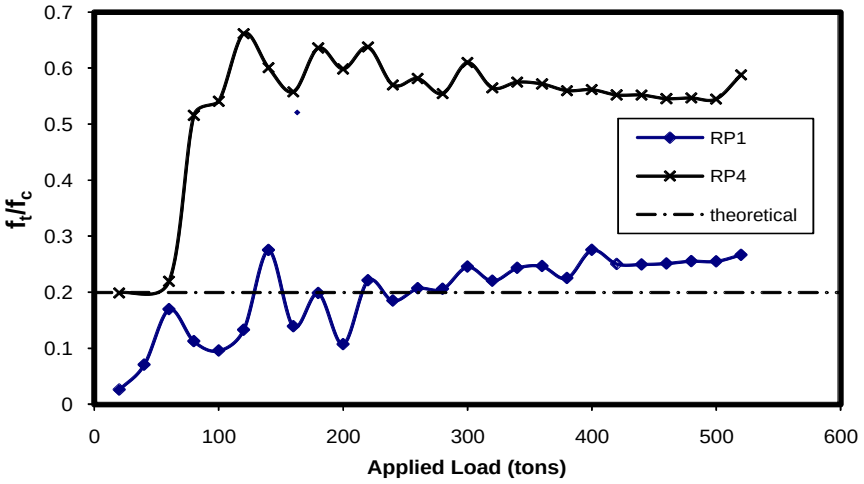

Figure 17 Measured and Predicted Side Friction Ratio in Hard Clay – CB (Clay Site)

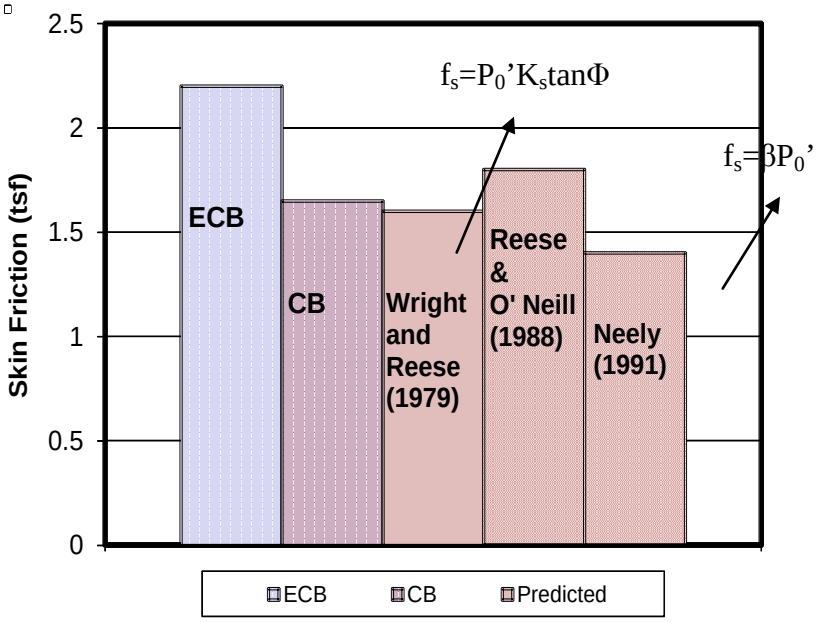

Figure 18 Comparison of Measured and Predicted Skin Friction

End Bearing of the Test Pile

End bearing of the pile from the linearly extrapolated toe load. The load was divided with the nominal cross sectional area to get the unit base resistance at the toe of the pile. The relationship between the base resistance, q and toe settlement, w for both the test pile was shown in Figure 19. The end bearing of the dense sand and hard clay was 8.2 tsf and 31 tsf respectively. End bearing developed in the hard clay was 2.5 times greater than the dense sand for approximately at the same displacement. The end bearing in the dense sand at a displacement of 0.29 in. was 8.2 tsf, whereas in the hard clay layer the end bearing was 21.8 tsf at 0.3 in. displacement. End bearing in the clay was higher because of the high stiffness of the hard clay soil. High end bearing was also due to the construction effects in the dense sand layer soil was disturbed more, whereas in the case of stiff clay augered pile causes fewer disturbances to the surrounding soil than other types of piles because it was constructed by placing concrete in the augered hole and curing it in place (Ellison et al. (1971)

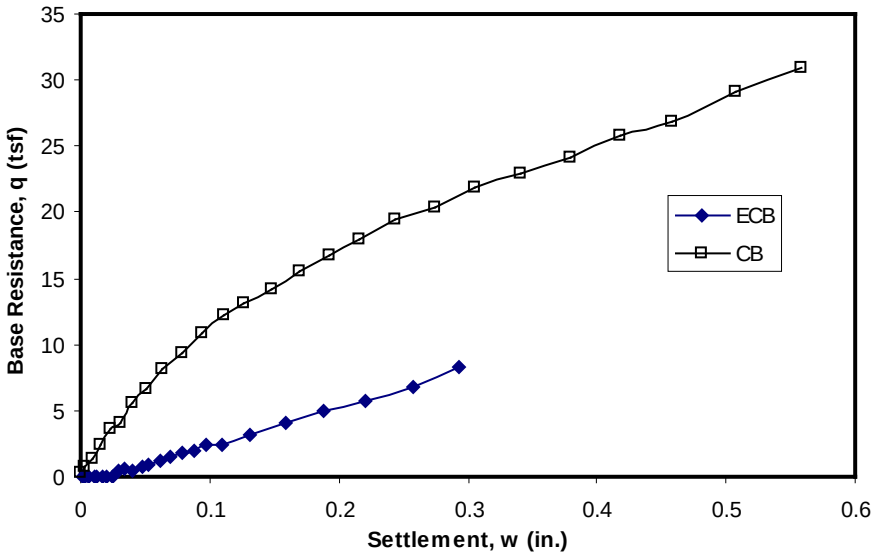

Figure 19 Base Resistance of the Test Piles

Design Methods of ACIP Pile

The ultimate axial capacity of an ACIP pile can be evaluated using the following equation which is simply the summation of side and toe resistance,

$$Q_t = Q_s + Q_p, \quad (1)$$

where

Q_t = total capacity,

Q_s = side resistance (skin friction) capacity,

Q_p = toe resistance (end bearing) capacity.

The general equation for side resistance can be stated as

$$Q_s = f_{sa}\, \pi\, DL, \quad (2)$$

where

f_{sa} = Average unit side resistance over embedded length L of pile.

D = diameter of pile.

L = Length of penetration of pile in ground.

The general equation for toe (tip, base) resistance can be written as

$$Q_p = q_p\, A_p, \quad (3)$$

where

q_p = Ultimate unit toe resistance

A_p = Toe area of pile.

Because the axial load-displacement behavior of the ACIP piles is between driven piles and drilled shafts, proposed methods to estimate the ACIP pile capacity may be based on either driven pile or drilled shaft design methods. Various design methods proposed for Auger Cast in Place (ACIP) piles are summarized in Table 1

Table 1 Design Methods for ACIP Pile

Sl No	Design Methods	Type of Soil	Side Resistance	Toe Resistance	Remarks
1	Coyle & Castello (1981)	Clay	$f_{sa} = \alpha\ s_{ua}$ $\alpha = 0.2$ to 1.0	$q_p = 9\ s_u$	Based on database of 16 load tests
2	LPC Method (Bustamante & Gianeselle (1982)	Layered Soil	$Q_s = \Sigma\Delta Q_{st} = \Sigma A_{si} f_{si}$ ΔQ_{st}= side resistance for each layer	Cohesionless Soil $q_p = 0.15\ q_c$ Cohesive Soil $q_p = 0.375\ q_c$	Based on CPT values
3	Douglas Method (1983)	Sand	$f_{sa} = P_0' K_s \tan\varphi \leq$ 0.15 MPa (1.6 tsf)	25% of CPT value at pile tip level	Based on load tests on ACIP piles
4	FHWA (Reese & O'Neill, 1988)	Cohesive & Cohesion-less Soil	Cohesive Soil $f_{max}=0.55 s_u$ Cohesionless Soil $f_{max}=K_z \sigma'_{vz} \tan\delta_z = \beta_z \sigma'_{vz}$ $\beta_z = K_z \tan\delta_z = 1.5 - 0.135(z)^{0.5}$, $(0.25 \leq \beta_z \leq 1.2)$	Cohesive Soil $q_{max}=N_c s_u$ (N_c=9) Cohesionless Soil q_{max}(tsf)=0.6 $N_{SPT} \leq 30$ tsf	Based on database of drilled shaft loading tests
5	Rizkallah Method (German Standard, 1988)		0.8% of the average CPT value for each layer	q_{ult} is calculated for a settlement equal to 5% of the pile diameter	Based on CPT values
6	Neely Method (1991)	Sand	$f_{sa} = \beta P_0' \leq$ 0.135 MPa (1.4 tsf), $\beta = K_s \tan\delta$,	q_p (tsf) = 1.9 N$\leq$ 7.2 MPa (75 tsf)	Based on a database of 66 load tests on ACIP pile for sandy soil

Table 1 Design Methods of ACIP Pile (Contd)

7	Viggiani (1993)	Cohesion-less Soil of volcanic origin	f_{sa} = f(CPT)α α = dimensionless factor	q_{ult} is calculated for a settlement equal to 25% of the pile diameter	Based on load tests on soils of volcanic origin
8	Wright & Reese (1997)	Sand	f_{sa}= P_0'$K_s$tanφ ≤ 0.15 MPa (1.6 tsf)	q_p = 2/3 N≤ 3.8 MPa (40 tsf)	Based on the ultimate capacity of drilled shafts in sand
9	Zelada & Stephenson (2000)	Cohesion-less Soil	f_s= βP_0' β = 1.2 – 0.108$z^{0.5}$ (0.2≤ β_z ≤1.96)	q_b= 1.7 N≤ 75 tsf	Based on database of 53 pile tests.
10	Vipulanandan Method (2004)	Mixed Soil	$Q_{ult}/LD=0.019q_c+0.2=\frac{q_c}{7.8+1.9q_c}$ $\frac{\rho_{50}}{d}\%=\frac{0.015}{f_s/q_c}$		Based on CPT tests of different soils in Texas, Gulf Coast.
11	Kulhawy & Chen (2005)	Cohesion-less soil	$Q_{L2}\approx Q_{STC}$ Q_{L2}=failure threshold or interpreted failure load Q_{STC}=Slope tangent load		Based on database of 56 load tests Load-displacement behavior
12	Vipulanandan et al. (2005)	Cohesive Soil	$\frac{Q}{Q_{ult}}=\frac{\rho/d}{\rho_{50}/d+\rho/d}$		Predict the load-displacement behavior

where

P_o' = Avg. effective vertical stress along pile,

Ks = Lateral earth pressure coefficient,

ϕ = Angle of internal friction of sand.

su = the undrained shear strength of the clay layer

Asi = πDΔLi, and

ΔLi = length of the pile in layer i

qc = Cone resistance.

Kz = coefficient of lateral pressure at depth z,

σ'vz = vertical effective stress in the geomaterial at depth z,

z = depth below the ground surface,

δz = friction angle between concrete and soil at depth z

Nc = a bearing capacity factor taken as 9

δ = internal friction angle at pile-soil interaction

L = length of the pile.

D = diameter of the pile.

ρ_{50} = displacement at the half of the ultimate load.

d = diameter of the pile.

f_s = side resistance of the cone.

q_c = tip resistance of the cone.

Load Test Database and Modeling

A database of 15 full-scale load-displacement behaviors of ACIP piles in cohesive soils and cohesionless soils with diameters ranging from 14 to 30 in. and length varying from 12 to 93 ft from many parts of Texas was investigated. The measured pile capacities varied from 90 to 410 tons. Based on the observed trends a non-dimensional hyperbolic relationship wereused to verify the non linear load-displacement behavior of full scale load test data. In buildings and bridges displacement of piles is important criteria, and hence it is important to determine the load-displacement relationship for the piles (Vipulanandan et al., 2005). But most of the load tests are performed to a load twice or thrice of the design load and not to the complete failure of the pile. Ultimate capacity criteria such as load at 5% or 10% of diameter of pile or Davisson's criterion (Davisson, 1972) are used to predict the ultimate capacity of the pile. Hence it is necessary to develop the representative models for load-displacement relationships for ACIP piles.

Cohesive Soil

A total of 12 load tests, on ACIP piles in cohesive soil in Texas were studied. Load tests were performed using conventional static loading system in accordance with ASTM D1143, "Quick Load Test Method for individual piles". The displacement of pile head was measured with at least three dial gages supported on reference beam. Characterization of overburden soil in original boring log has been reported in terms of Pocket Penetrometer (PP) values or SPT (N blows / 300 mm). General information on all the load test sites was shown in Table 2. The diameter of the pile studied varied from 16 in. to 24 in. and the length varied from 12 ft. to 93 ft. As summarized in Table 2 seven of the load tests were performed to a displacement of less than 5% of the diameter of the pile.

Table 2 Load Test Results for ACIP Piles in Cohesive Soil

Case No	Location, TX	Type of pile	Diameter (in.)	Length (ft)	Max*. Load (kips)	Max. Displacement % D
1	Mc Allen	ACIP	16	45	480	4.13
2	Houston	ACIP	16	60	260	1.23
3	Houston	ACIP	16	60	320	4.69
4	Houston	ACIP	16	70	400	6.38
5	Freeport	ACIP	16	30.3	202	7.00
6	Freeport	ACIP	16	50	225	1.81
7	Bryan	ACIP	18	50	595.2	6.98
8	Paris	ACIP	16	45	300	4.86
9	Coppell	ACIP	24	35	440	2.48
10	Houston	ACIP	18	80	600	5.50
11	Houston	ACIP	18	68.5	315	2.31
12	Houston	ACIP	18	93	760	5.56
Range			16-24	12-93	45-760	1.8-7

Cohesionless Soil

A total of three load tests, on ACIP piles in cohesive soil in Texas were studied. General information on all the load test sites was shown in Table 2. The diameter of the pile studied varied from 14 in. to 30 in. and the length varied from 33 ft. to 75 ft. As summarized in Table 3 one of the load tests was performed to a displacement of less than 5% of the diameter of the pile.

Table 3 Load Test Results for ACIP Piles in Cohesionless Soil

Case No	Location, TX	Type of pile	Diameter (in.)	Length (ft)	Max*. Load (kips)	Max. Displacement % D
1	Houston	ACIP	14	75	1080	5.95
2	Galveston	ACIP	18	50	386	8.81
3	Crockett	ACIP	30	33	640	1.2
Range			14-30	33-75	386-1080	1.2-8.81

Ultimate Capacity

One mathematical relationship that will satisfy the ACIP pile behavior is the two parameter hyperbolic relationship (Vipulanandan et al 2005) which can be represented as

$$Q = \frac{\rho}{A + B\rho}, \tag{4}$$

Chin (1970) has used hyperbolic relationships to estimate the ultimate capacity of piles, when load tests did not reach failure load and to investigate defects in driven piles. By rearranging the Eqn. (5) to represent a linear relationship

$$\frac{\rho}{Q} = A + B\rho, \tag{5}$$

where

Q = Load

ρ = Settlement

A and B are constants which can be obtained from the linear relationship.

All the pile test data were verified by the linear relationship (Eqn. (5)) within an acceptable limit (high coefficient of correlation). The agreement was very good. Parameters A and B was obtained from the linear relationship for further analyses. Figure 20 shows the typical plot of ρ / Q versus ρ. The coefficient of correlation was 0.99. Similar trend was observed with all the piles. Figure 21 shows the typical load displacement behavior of ACIP pile. The model parameters were obtained from the hyperbolic relationship. The hyperbolic relationship was in good agreement with the measured data. When the displacement becomes large the pile capacity reaches its theoretical maximum (Q_{ult}) and it will be related to parameter B

$$Q_{ult} = \frac{1}{B} \tag{6}$$

The ultimate capacity for each case was determined and the $Q_{measured}$ to Q_{ult} ratio varied from 0.50 to 0.95.

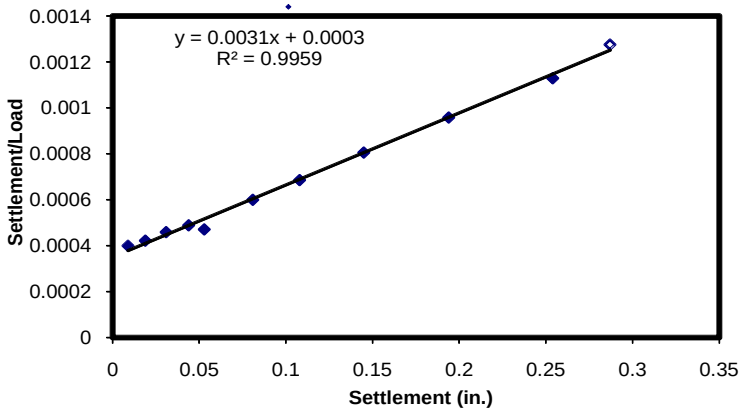

Figure 20 Typical Plot of ρ / Q Vs ρ

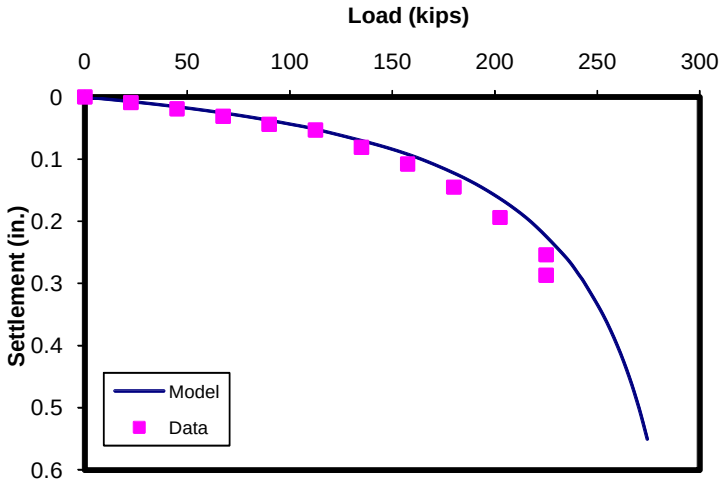

Figure 21 Load-Displacement Behavior

Load-Displacement Relationship

As summarized in Table 2 and Table 3 some of the load tests were performed to a displacement of less than 5% of diameter and hence a model should be used to best estimate the ultimate capacity of the piles at appropriate deflection. Vipulanandan et al (2005) have used the non-dimensional hyperbolic relationship to predict the load-displacement behavior of ACIP piles in soils. The non-dimensional form of hyperbolic relationship is given by

$$\frac{Q}{Q_{ult}} = \frac{\rho/d}{\rho_{50}/d + \rho/d} \qquad (7)$$

where ρ_{50}/d is the displacement to diameter ratio for Q/Q_{ult} ratio of 0.5. The ratio ρ_{50}/d for ten ACIP piles in cohesive soils except for one, varied from 0.3% to 1.85% as shown in

Figure 22. For the cohesionless soil the ratio was 0.48% to 2.0% (Figure 23). Earlier studies based on ten load test data on cohesive soils showed that the ratio ρ_{50}/d was in the range of 0.3 to 2% (Vipulanandan et al. 2009).

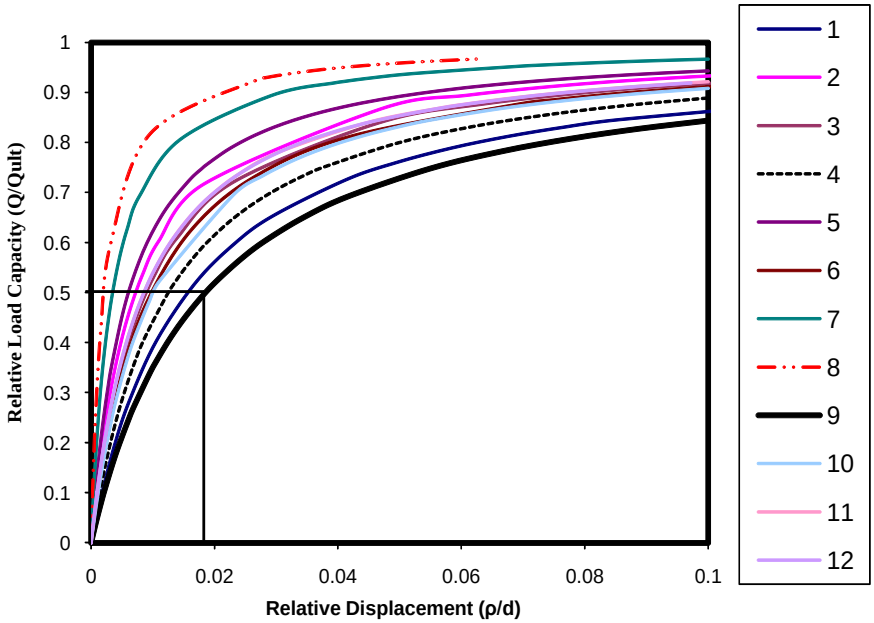

Figure 22 Variations of Relative Displacement and Relative Load Capacity for Cohesive Soil

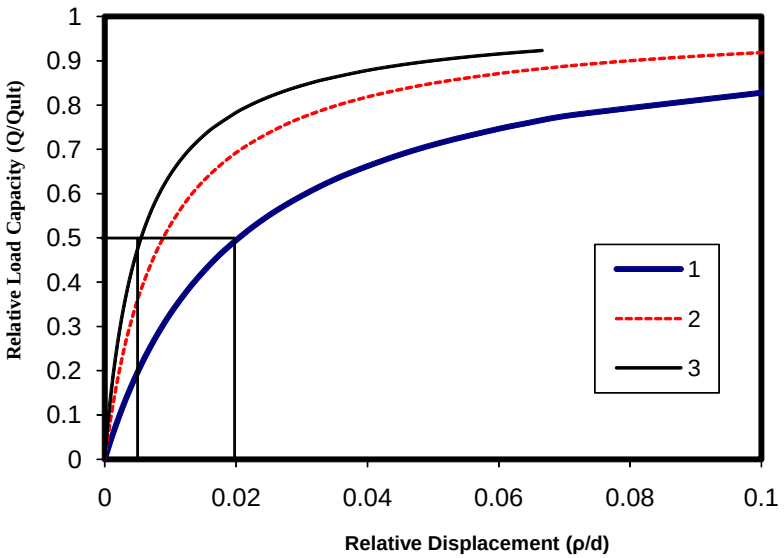

Figure 23 Variations of Relative Displacement and Relative Load Capacity for Cohesionless Soil

Conclusions

Based on the monitoring and the field tests on ACIP piles the following conclusions are advanced

1. Monitoring the construction and curing of the grout will be helpful in determining the quality of the pile and also to decide the right time to perform a load test or to continue on the super structure construction. The average time to reach the maximum temperature in the dense sand was 8.4 hrs, whereas the average time to reach the maximum temperature in the clay was 9.4 hrs.
2. End bearing developed in hard clay was 2.5 times higher than the end bearing developed in dense sand for the same displacement (1% D) due to the higher stiffness of the hard clay soil.
3. The maximum side friction measured in compression was 2.2 tsf and that measured in tension was 0.6 tsf in sand. The maximum side friction in the hard clay was 1.65 tsf in compression and the side friction measured in tension was 0.8 tsf. Side friction in the dense sand was 1.8 times greater than the side friction in the hard clay for the same displacement at 1% D.
4. Based on the load testing the measured pile load at 1.2% D displacement at the clay site (CB) was 1.2 times the measured load at the sand site (ECB).
5. The ratio of ρ_{50}/d varied from 0.3% to 1.85% for most of the ACIP piles in cohesive soils. For the ACIP piles in cohesionless soil the ratio of ρ_{50}/d varied from 0.48% to 2.0%.

Acknowledgement

This study was supported by CIGMAT with partial funding from various industries. Sponsors are not responsible for any of the findings. The pile load test data provided by Berkel and Company is gratefully acknowledged.

References

Brown, D. A. (2005). “Practical Considerations in the Selection and Use of Continuous Flight Auger and Drilled Displacement Piles,” Geotechnical Special Publication No. 132, ASCE, pp. 1-11.

Bustamante, M. and Gianeselli, L. (1982). “Pile Bearing Capacity Prediction by Means of Static Penetrometer.” Proc. 2nd Eur. Symp. On Penetration Testing, Esopt II, Amsterdam. 493-500.

Chin, F. K. (1970), “Estimation of the Ultimate Load of Piles from Tests not carried to Failure.” Proc., 2nd South East Asian Conference on Soil Engineering, Singapore, 81-90.

Coyle, H.M. and Costello, R. (1981) “New Design Correlations of Piles in Sand,” Jl. of Geotech. Engrg., ASCE , 107(GT 7), 965-986.

Davisson, MT (1972). "High Capacity Piles," Proc., Lecture Series Innovations in Fndn. Construction, ASCE Illinois Section, Chicago, 52 p.

DFI (1994). “Augered Cast-In-Place Piles Manual,” Deep Foundations Institute, Sparta, NJ.

Douglas, DJ (1981). “Design of Augered Grouted Piles,” Proc. Symp. Grout Injected Piles, Brisbane, 2.1-2.21.

Neate, JJ (1988). “Augered Cast-In-Place Piles,” Proc., 13th Annual Members’ Conf., Deep Fndns. Inst., Atlanta, 167-175.

Neely, W. J. (1991). “Bearing Capacity of Auger-Cast Piles in Sand,” Jl.of Geotech. Engrg., ASCE 117(2), 331-345.

O’Neill, M. W. (1994). “Review of Augered Pile Practice Outside the United States,” Transportation Research Record No. 1447, TRB, Washington D. C, 3-9.

Reese, L. and O’Neill. M. (1988). Drilled Shafts, Publication FHWA-HI-88-042. FHWA, U. S Department of Transportation.

Rizkallah, V., (1988). “Comparison of Predicted and Measured Bearing Capacity of Auger Piles.” Deep Foundations on Bored and Auger Piles, BAP I, Balkema, Rotterdam, pp. 471-475.

Vigginai, C. (1989). "Influenza dei fattori tecnologici sul compartamento dei pali." Atti. XVII Convegno Nazionale di Geotecnica. Taormina, Vol. 2, pp. 83-91

Viggiani, C. (1993). “Further Experiences with Auger Piles in Naples Area,” Proc. first Intl. Geotech. Seminar on Deep Foundations on Bored and Auger Piles, Ghent. 445-458.

Vipulanandan, C., Tand, K. E. and Kaulgud, S. (2005) "Axial Load-Displacement Relationship and CPT Correlation for ACIP Piles in Texas Gulf Coast Soils," Proc., Advances in Designing and Testing Deep Foundations, GSP 129, ASCE Geo Institute, 290-308.

Vipulanandan, C., Guvener, O. and McClelland M. (2007). “Monitoring and Curing of a Large Diameter ACIP Piles in Very Dense Sand,” CD Proceedings (CD), GSP 158, Contemporary Issues in Deep Foundations, ASCE Geo Institute.

Wright, S. J and Reese, L. C. (1979). “Design of Large Diameter Bored Piles.” Ground Engrg, London, UK, 12(8), 47-51.

Zelada, G.A., and Stephenson, R.W. (2000). “Design Methods for ACIP Piles in Compression,” New Technological and Design Developments in Deep Foundations, ASCE GSP 100, 418-432.